



Size-resolved aerosol pH over Europe during summer

Maria Zakoura^{1,2}, Stylianos Kakavas^{1,2}, Athanasios Nenes^{1,3} and Spyros N. Pandis^{1,2,4}

¹Institute of Chemical Engineering Sciences, ICE/FORTH, Patras, Greece,

5 ²Department of Chemical Engineering, University of Patras, Patras, Greece,

³Ecole Polytechnique Fédérale de Lausanne (EPFL), Switzerland

⁴Department of Chemical Engineering, Carnegie Mellon University, Pittsburgh, USA

10 *Correspondence to:* Spyros N. Pandis (spyros@chemeng.upatras.gr) and Athanasios Nenes (athanasios.nenes@epfl.ch).

Abstract. The dependence of aerosol acidity on particle size, location and altitude over Europe during a summertime period is investigated using the hybrid version of aerosol dynamics in the chemical transport model PMCAMx. The pH changes more with particle size in northern and southern Europe owing to the enhanced presence of non-volatile cations (Na, Ca, K, Mg) in the larger particles. Differences of up to 1-4 pH units are predicted between sub- and super-micron particles, while the average pH of PM_{1-2.5} can be as much as 1 unit higher than that of PM₁. Most aerosol water over continental Europe is associated with PM₁, while PM_{2.5-5} and PM₅₋₁₀ dominate the water content in the marine and coastal areas due to the relatively higher levels of hygroscopic sea salt. Particles of all sizes become increasingly acidic with altitude (0.5-2 units pH decrease over 2.5 km) primarily because of the decrease in aerosol liquid water content (driven by humidity changes) with height. Inorganic nitrate is strongly affected by aerosol pH with the highest average nitrate levels predicted for the PM_{2.5-5} range and over locations where the pH exceeds 3. Dust tends to increase aerosol water levels, aerosol pH and nitrate concentrations for all particle sizes. This effect of dust is quite sensitive to its calcium content. The size-dependent pH differences carry important implications for pH-sensitive processes in the aerosol.

15
20
25

1. Introduction

Acidity is an aerosol property of central importance driving gas-particle partitioning and heterogeneous chemistry (Pye et al., 2019). pH affects the formation of semi-volatile particulate matter and the nitrogen cycle by modulating HNO₃/NO₃⁻ and NH₃/NH₄⁺ gas-particle partitioning (Meskhidze et al., 2003; Guo et al., 2017; Nenes et al., 2019). Aerosol acidity can influence pH-

30



dependent heterogeneous atmospheric processes, like oxidation of SO₂ to sulfate, formation of secondary organic aerosol and uptake of N₂O₅ on particles (Huang et al., 2011) and also influences
35 aerosol hygroscopicity (Hu et al., 2014). Deposition of acidic particles causes damage on building materials, forests, and aquatic ecosystems (Xue et al., 2011). Aerosol pH can change the solubility of metals, such as iron and copper, which have been linked to aerosol toxicity, and at the same time affects nutrient distributions with impacts on photosynthesis productivity and ocean oxygen levels (Meskhidze et al., 2003; Nenes et al., 2011). Adverse health outcomes have been linked to aerosol
40 acidity, including respiratory diseases (Raizenne et al., 1996), oxidative stress (Fang et al., 2017) and lung and laryngeal cancers (Hsu et al., 2008).

The nitrate partitioning to the aerosol phase is favored when pH exceeds a threshold value (between 1.5 and 3) that depends logarithmically on liquid water content and temperature (Meskhidze et al., 2003; Guo et al., 2016; Nenes et al., 2019). If aerosol pH is high enough
45 (typically above 2.5 to 3), aerosol nitrate formation is favored, as most of the total nitrate formed from NO_x chemistry resides in the aerosol phase. For lower pH values (below 1.5 to 2), formation of aerosol nitrate is not favored and remains in the gas phase as HNO₃. Between these pH value limits, a sensitivity window (of 1 to 1.5 pH units) exists in which nitrate can be found either as gas or as aerosol (Vasilakos et al., 2018; Nenes et al., 2019). Atmospheric aerosol has often pH values inside
50 this sensitivity window, for which pH errors could translate to importance biases in aerosol composition (Bougiatioti et al., 2016; Guo et al., 2015, 2017; Vasilakos et al., 2018).

Aerosol acidity and partitioning of semi-volatile species, like nitrate, can be modulated by the presence of soluble inorganic cations of sea salt and mineral dust, such as Na⁺, K⁺, Ca²⁺ and Mg²⁺ (Vasilakos et al., 2018). These non-volatile cations (NVCs) tend to reside in the coarse mode
55 of ambient aerosol (sea salt, dust), with much lower concentration in smaller particles (Seinfeld and Pandis, 2006). Chemical transport models tend to overpredict aerosol inorganic nitrate levels in both US and Europe (Yu et al., 2005; Pye et al., 2009; Fountoukis et al., 2011; Tuccella et al., 2012; Heald et al., 2012; Walker et al., 2012; Im et al., 2015; Ciarelli et al., 2016; Zakoura and Pandis, 2018; Zakoura and Pandis, 2019). One of the reasons for these errors is that these models do not
60 simulate properly the aerosol acidity introducing errors in gas-particle partitioning of semi-volatile species, often affecting predictions of inorganic nitrate (Vasilakos et al., 2018).

The aerosol pH has been estimated combining field measurements and aerosol thermodynamic models. Katoshevski et al. (1999) estimated the aerosol pH in the marine boundary layer using the thermodynamic model ISORROPIA and found that it ranged between -0.5 to 9 for
65 particle diameters smaller than 1 μm up to 10 μm. pH was estimated to be 0 to 2 for the



accumulation mode and 2-5 for the coarse mode particles using aerosol and gas phase data collected over the Southern Ocean in combination with the EQUISOLV II model (Fridlind and Jacobson, 2000). Keene et al. (2004) calculated mean pH, ranging from 2.6 to 3.9, for 0.75-25 μm particles based on measurements by an impactor for aerosols and Teflon filters for gases in New England during summer. $\text{PM}_{2.5}$ pH was calculated with ISORROPIA II in Beijing during all seasons in 2016-2017 with values ranging from 3.8 to 4.5 (Ding et al., 2019). $\text{PM}_{2.5}$ particles are strongly acidic in Hong Kong, China ($[\text{H}^+]=103 \text{ nmol m}^{-3}$ for spring of 2001) (Pathak et al., 2003). $\text{PM}_{2.5}$ particles during different seasons at an urban site in Guangzhou, China were generally acidic (average $[\text{H}^+] \sim 70 \text{ nmol m}^{-3}$) (Huang et al., 2011). Guo et al. (2015) estimated that PM_1 particle pH varied from 0.5 to 2 in the summer and 1 to 3 in the winter in the Southeastern US. PM_1 pH was estimated for the northeastern US and its mean value was 0.77 (Guo et al., 2016). $\text{PM}_{2.5}$ pH values of 0-2 were estimated combining ISORROPIA II and data collected at a rural southeastern US site during summer 2013 (Weber et al., 2016). Based on impactor measurements in Atlanta, GA during the spring of 2015, Fang et al. (2017) calculated a mean pH value of 3.5 for the coarse mode particles using the ISORROPIA II model. Guo et al. (2017) calculated PM_1 and $\text{PM}_{2.5}$ pH (equal to 1.9 and 2.7) from measurements during the CalNex study in combination with ISORROPIA II. An average PM_1 pH equal to 2.2 was estimated in a rural southeastern US site using ISORROPIA II (Nah et al., 2018). Vasilakos et al. (2018) used the three-dimensional chemical transport model, CMAQ, along with ISORROPIA II, to predict the annual average $\text{PM}_{2.5}$ pH over the Eastern US for 2001 and 2011 (pH equal to 1.6 and 2.5, respectively). Bougiatioti et al. (2016) calculated PM_1 pH (between -0.97 and 3.75) using ISORROPIA II in the eastern Mediterranean. Squizzato et al. (2013) estimated a mean $\text{PM}_{2.5}$ pH value equal to 3.1 over Po Valley, Italy during 2009 based on filter measurements using the E-AIM thermodynamic model. A comprehensive survey of pH studies to date can be found in Pye et al., (2019).

Most of the previous studies focused on the average pH of a particular size range neglecting potential pH variation with particle diameter. There is evidence that pH may vary by as much as 6 units between particle diameters of 0.1 μm to 10 μm (Fang et al., 2017; Ding et al., 2019). The majority of previous work has focused on select locations in the US, Canada and Asia and there is still little information about Europe. Also, there is only one study that links aerosol acidity with altitude (Guo et al., 2016), indicating the need for further investigation.

The aim of our work is to investigate the size-dependent aerosol pH over Europe. For this purpose, the Particulate Matter Comprehensive Air quality Model with extensions, PMCAMx, including the thermodynamic model ISORROPIA II, was used. Europe is particularly interesting,



owing to the large concentration of NH_3 , nitrate, sulfate and dust across all sizes. The role of dust,
100 Ca^{2+} and the variation of aerosol pH with altitude are analyzed in detail.

2. Model description

PMCAMx (Tsimpidi et al., 2010; Karydis et al., 2010) is based on the CAMx air quality model
(Environ, 2003) to simulate the processes of horizontal and vertical advection, horizontal and
105 vertical diffusion, wet and dry deposition, gas- and aqueous-phase chemistry. A sectional approach
is used to dynamically track the evolution of the aerosol mass and composition distribution across
10 size sections covering a diameter range from 40 nm to 40 μm . The aerosol components modeled
include sulfate, nitrate, ammonium, sodium, chloride, calcium, potassium, magnesium, other inert
crustal material, elemental carbon, water, primary and secondary organic species. The gas-phase
110 chemical mechanism used in this application is based on the SAPRC mechanism (Carter, 2000;
Environ, 2003). The version of SAPRC mechanism used here includes 237 reactions of 91 gases, 18
radicals and 37 aerosol species. The thermodynamics of inorganic species was simulated using the
ISORROPIA II model (Fountoukis and Nenes, 2007). Additional details regarding PMCAMx are
provided in Fountoukis et al. (2011).

115 We use the hybrid approach to model inorganic aerosol mass transfer, where for particles
with dry diameters less than 1 μm , bulk equilibrium is assumed. For larger particles, the mass
transfer to each size section is simulated using the Multicomponent Aerosol Dynamics Model
(Pilinis et al., 2000). Trump et al. (2015) used the hybrid approach over Europe to improve the
simulation of coarse particle chemistry. They found that PM_{10} nitrate overprediction in areas with
120 high sea-salt levels was reduced with the hybrid approach due to the more accurate representation of
the interaction of nitric acid and ammonia with coarse mode sea salt. These interactions result in
reduction of fine nitrate and increase of nitrate in the coarse mode. Given the importance of pH on
the partitioning of nitrate, the hybrid approach is essential for capturing the size-resolved variability
of pH.

125 pH is calculated in this work for particles smaller than 1 μm , 1-2.5 μm , 2.5-5 μm and 5-10
 μm , using a molal definition consistent with the pH_F definition of Pye et al. (2019):

$$\text{pH} = -\frac{\log(1000[\text{H}^+])}{[W]}, \quad (1)$$

where $[\text{H}^+]$ and $[W]$ are the concentrations of particle hydronium ion and particle water in $\mu\text{g m}^{-3}$.



130 3. Model application

PMCAMx was applied over Europe, during the EUCAARI summer intensive campaign in May 2008 for which the model has been evaluated in previous work (Fountoukis et al, 2011). The domain covers a 5400×5832 km² region with 36×36 km grid resolution and 14 vertical layers extending up to 6 km. Inputs to the model include horizontal wind components, vertical diffusivity, temperature, pressure, water vapor, clouds and rainfall, all generated using the Weather Research and Forecast (WRF) meteorological model (Skamarock et al., 2005). Anthropogenic gas-phase emissions include land emissions from the GEMS dataset (Visschedijk et al., 2007) as well as international shipping emissions. Anthropogenic particulate emissions of organic and elemental carbon were obtained from the EUCAARI Pan-European Carbonaceous Aerosol Inventory (Kumala et al., 2009). Industrial, domestic, agricultural and traffic emission sources are included in the two inventories. Biogenic emissions were based on MEGAN (Guenther et al., 2006), and sea-salt emission inventories were developed using the approach of O’Dowd et al. (2008). Urban dust emissions were based on the work of Kakavas et al. (2020), assuming that calcium, potassium, magnesium and sodium represented 2.4%, 1.5%, 0.9%, and 1.2% of the emitted mineral dust, respectively. A reliable Saharan dust emissions inventory was not available; therefore, the African region is excluded from the simulation analysis. More information about the inputs of PMCAMx during the simulated period can be found in Fountoukis et al. (2011) and Kakavas et al. (2020).

Three simulations were performed. The first was the “base case” simulation and included all emissions described above. Two other simulations are carried out and compared with the “base case” to understand how NVCs in dust affect water uptake and aerosol pH: one where dust lacks any non-volatile soluble cations (“inert dust” simulation) and one where we neglect calcium (the major NVC in dust) from the “base case” simulation. Calcium is unique compared to the other NVCs in that it can react with sulfate ions and form insoluble CaSO₄, which precipitates out of the aerosol aqueous phase and remains insoluble under subsaturated conditions - even for metastable aerosol (Fountoukis and Nenes, 2007). This unique interaction implies that Ca, if present in sufficient amounts, can reduce aerosol sulfate and reduce acidity, but at the same time reduce hygroscopicity that promotes acidity- in a way that is not obvious by just comparing the base case simulation with the “inert dust” simulation. In all simulations, the total dust mass emissions were the same and only its assumed composition varied.

160



4. Results and discussion

4.1 Size dependence of aerosol pH

165 The average ground level pH predictions for different size ranges are presented in Fig. 1. pH is
higher over the sea for all particle sizes compared to continental regions due to the presence of sea
salt, lower NH_3 and the systematically higher RH and liquid water content – all of which act to
reduce aerosol acidity. The pH of marine aerosol increases with particle size, with the highest value
equal to 4.5 for the 2.5-5 μm and 5-10 μm ranges, as sea salt is emitted mainly at the super-micron
170 range and is the main aerosol component. Over the continental region, average PM_1 pH ranges
between 1 to 3 with the highest values in the northern coastal parts of Europe and northern Italy; in
these regions, acidity is reduced by the high levels of NH_3 present from agriculture and livestock
emissions combined with high NO_x and RH levels (Guo et al., 2018; Masiol et al., 2019). $\text{PM}_{1-2.5}$ is
less acidic with pH values from 1 to 4 over the continental region with the higher values in the
175 northern coastal areas of Europe (e.g., parts of the United Kingdom). The average pH increases
further in the 2.5-5 μm range being equal to 2-3 over the continental regions and reaching values up
to 4-4.5 in the northern coastal areas of the United Kingdom, Belgium, France and Poland. Average
 PM_{5-10} pH slightly decreases over the continental region compared to $\text{PM}_{2.5-5}$, especially in central
Europe, and the highest pH values (4-4.5) predicted for the same regions. The size-dependence of
180 pH is stronger in the northern and southern parts of Europe, and weaker in central Europe, in which
the average pH is in the 1.5-3 range for all particle sizes. The largest pH changes across size occur
for regions where fine-mode aerosol acidity is dominated by the $\text{NH}_3\text{-SO}_4$ system (i.e., relatively
lower NH_3 levels – so that aerosol nitrate is low; Guo et al., 2018), and the largest sizes contain
large amounts of NVCs from sea salt and dust.

185 Squizzato et al. (2013) calculated $\text{PM}_{2.5}$ pH equal to 2.3 and Masiol et al. (2019) equal to 2.2
in the Po Valley, Italy during the summer of 2009 and 2012, respectively. The PMCAMx
predictions for this area are in good agreement with these studies, as $\text{PM}_{2.5}$ pH is predicted to be
equal to 2.4. Guo et al. (2018) estimated that the $\text{PM}_{2.5}$ pH was equal to 3.3 in Cabauw, Netherlands
during summer 2013, based on measurements and thermodynamic modeling. PMCAMx
190 underpredicts $\text{PM}_{2.5}$ pH by 0.8 units (equal to 2.5) in this area during the summer. Part of this
discrepancy could be due to the different periods compared. Bougiatioti et al. (2016) determined
through thermodynamic analysis of observations with ISORROPIA-II that the PM_1 pH in Finokalia,
Crete is equal to 1.3 which agrees within 0.4 units with our predictions (equal to 1.7).

The pH of $\text{PM}_{2.5}$ has often been the focus of previous measurement studies, due to the
195 availability of the corresponding filter samples. However, the pH in the 1-2.5 range can be quite



different from that in the sub-micrometer range (Fang et al., 2017; Ding et al., 2019). This difference may have important implications for aerosol toxicity, metal solubility, nitrate partitioning and other processes. The difference of average ground level aerosol pH predictions between $PM_{1-2.5}$ and PM_1 is shown in Fig. 2. The pH of these size ranges can differ up to 1 unit over the continental region.
200 This difference is even higher over the ocean (up to 1.4 units), owing to the effect of NVCs from sea-salt levels.

Particle water concentrations for the different particle sizes are shown in Fig. 3. PM_1 has the most water, compared to the other size fractions over the continental region. The coarse particles in $PM_{2.5-5}$ and PM_{5-10} have the most water over sea owing to sea salt, which is found in higher levels in
205 these particles, and exhibits the highest hygroscopicity – compared to all other inorganic salts found in aerosol. Water levels for all particle sizes are higher at areas closer to the sea, owing to the relatively high dry aerosol mass concentration combined with the high RH typically associated with the marine environments; in just the 2.5-5 μm size range alone, water content exceeds 20 $\mu\text{g m}^{-3}$.

210 4.2 Temporal evolution of pH

To study the temporal evolution of pH, eight sites (Fig. S1) with different characteristics were selected based on their different type, location and dust/sea salt levels (Table S1). Iza, in Ukraine, has the lowest PM_1 pH of all examined locations with a value equal to 0.25 (Fig. S2). The pH is predicted to vary between -0.5 and 1.4 (on an hourly basis) in this region of Eastern Europe that is
215 characterized by high sulfate levels. Mace Head, on the other hand, has the highest average PM_1 pH (1.7) with values ranging between 0.9 and 2.3. Finokalia has the most variable PM_1 pH with a range covering 4 units. This site is affected by both relatively dry air masses with continental aerosol characteristics (low pH) and by air masses with relatively high sea-salt and dust levels as well as biomass burning influences (higher pH; Bougiatioti et al., 2016). The distribution of pH values of
220 the 1-2.5 μm diameter particles moves to higher values (less acidic particles) for all sites compared to the sub-micrometer particles. The pH values of all sites for the 2.5-5 μm range are similar to those in the 5-10 μm range and higher than the fine aerosol pH values.

The pH diurnal profiles for Cabauw, Melpitz, Paris, Finokalia are shown in Fig. 4. These sites were selected based on their different type, location and dust/sea salt levels (Table S1) – and
225 because ambient pH data is available for both of them (Pye et al., 2019). pH follows the same trend for all particle sizes in each of the four sites. Cabauw is characterized by relatively constant average diurnal pH with slightly higher values early in the morning. The average hourly pH is a lot more variable in Melpitz and Paris, with a peak early in the morning (up to 3.5 for Melpitz and 3.8 for



Paris), and then decreasing values during the day reaching a minimum in the afternoon. The pH
230 diurnal profile is different in Finokalia, since pH has its peak (up to 3.6) at noon (between 15-16
UTC time) and then starts to decrease. These variations are caused by a variety of factors including
the relative humidity (that is higher during the early morning, leading to higher liquid water content
and higher pH), the temperature (which tends to evaporate nitrate) and mixing height variation
(which in turn tends to affect precursor concentrations).

235

4.3 pH variation with height

All the results presented so far are for the ground level (lowest 50 m). The predicted aerosol water
content for all size ranges decreases with altitude (Fig. S3). This is mainly due to the decrease of the
relative humidity and aerosol concentrations with altitude (Mishra et al., 2015; Wang et al., 2018).
240 As height increases, pH values for all particle sizes decrease, due to the reduction of aerosol water
per unit mass of dry aerosol, with height (Fig. 5) – which is exclusively an effect of relative
humidity decrease. A secondary effect is that the lower concentration of aerosol tends to drive
partitioning of semi-volatile species (nitrate, ammonium) to the gas phase (Nenes et al., 2019). As a
result, particles of all sizes that are acidic at ground level become more acidic when they move
245 higher in the atmosphere.

For PM_{10} , in the less acidic areas over Europe the pH decreases from 2-2.5 near the ground to
around 1.5-2 at 2.5 km altitude. For $PM_{1-2.5}$, the reduction is even larger, since the pH values
decrease from 3-3.5 at the ground to 1.5-2.2 at 2.5 km (the larger drop in pH is a result of the
evaporation of nitrate aerosol and the decrease of liquid water content). Similar decreases of 1-1.5
250 pH units are predicted for the coarse particles in the first 2.5 km of the atmosphere in areas over
land. The predicted decrease in aerosol water content and pH for the super-micrometer particles is
even more pronounced in the marine atmosphere and coastal areas due to the high levels of sea-salt
near the ground. This reduction of pH with altitude is smaller for the PM_{10} size range in the marine
atmosphere.

255

4.4 Effect of aerosol pH on inorganic nitrate

The highest average nitrate levels ($0.7 \mu\text{g m}^{-3}$) are predicted for the 2.5-5 μm size range (Fig. S4) for
the whole domain. This size range is characterized by the highest average pH (with a value of 2.63).
Nitrate partitioning to the aerosol phase is favored when the aerosol pH is higher than 2.5 (Guo et
260 al., 2016; Vasilakos et al., 2018). At the same time, the mass transfer of the produced nitric acid in
the gas phase is faster for the particles in the 2.5-5 μm range compared to those in the PM_{5-10} range



also contributing to higher concentration. Finally, the removal of the larger particles from the atmosphere is faster adding one more reason for the maximum of the nitrate size distribution.

The size-dependent average nitrate diurnal profiles for Cabauw, Melpitz, Paris, and Finokalia, are shown in Fig. 6. In Cabauw, predicted total nitrate levels start to increase early in the morning, have their peak at noon or afternoon and decrease during the afternoon and early evening. Most of this variation is due to the formation of ammonium nitrate in the PM_{10} size range. The increase in PM_{10} nitrate is accompanied by an increase in the ammonium levels (Fig. S5) in this area that is characterized by high ammonia concentrations. The morning increase in the PM_{5-10} nitrate levels is due to the formation of sodium nitrate and calcium nitrate during daytime. In Cabauw, all super-micron particles have pH above 2.5, favoring the partitioning of nitrate to the aerosol phase forming also ammonium nitrate. In Melpitz, the behavior of nitrate is quite different than in Cabauw due to the differences in the pH behavior (Fig. 4). PM_{10} nitrate peaks early in the morning with peaks in coarse nitrate a few hours later. The peak in fine nitrate is at the same period as the pH in this range, while for the coarse particles it is a few hours later due to the delays in mass transfer to the larger particles. Nitrate levels in all size ranges are predicted to decrease during the afternoon with nitrate reaching a minimum in the late afternoon. The behavior of nitrate in the fine and coarse particles in Paris is quite similar as in Melpitz reflecting the similarity in the behavior of pH. Nitrate in all size sections peaks in the early morning and has a minimum in the afternoon. The main difference in this case is that there is more nitrate in the coarse particles due to the higher predicted levels of dust. In Finokalia, the predicted nitrate increases gradually in all sizes during the morning, reaches its maximum values in the afternoon and then gradually decreases.

4.5 Effect of dust on particle pH

The impact of the NVCs from dust on pH can be quantified comparing the results of the simulation in which the dust was assumed to be inert with the base case simulation. Aerosol water levels are higher in all particle sizes for the base case simulation (Fig. S6) compared to the inert dust simulation, as result of the water uptake associated with the NVCs. Dust is predicted to cause an increase of 1.2-2 $\mu\text{g m}^{-3}$ in aerosol water concentration even for the submicrometer particles over Europe with the highest changes in the northern areas. The water increases for $PM_{1-2.5}$ due to dust varies from 1 to 2.5 $\mu\text{g m}^{-3}$ over continental region. The effect, as expected, is higher for $PM_{2.5-5}$ reaching up to 3 $\mu\text{g m}^{-3}$ in areas like the Po Valley in Italy and even higher for PM_{5-10} ranging between 1 and 6 $\mu\text{g m}^{-3}$. The highest differences in aerosol water levels between the two simulations



are predicted for areas that combine relatively high values of RH and relatively high values of dust
295 (Fig. S7) during the simulated period.

The predicted aerosol pH is lower in all particle sizes for the inert dust case compared to the
base case simulation (Fig. 7). The soluble NVCs in dust tend to increase pH, as due to their lack of
volatility they irreversibly neutralize bisulfate ions that are generated by the $\text{NH}_3/\text{NH}_4^+$ equilibrium,
and therefore elevate aerosol pH. NVCs also elevate aerosol water in a way that leads to pH
300 increase, directly through their hygroscopicity and indirectly, through promoting the condensation of
aerosol nitrate (and its associated water content; Guo et al., 2018). PM_1 is also affected, even though
it contains small amounts of dust, as its pH increase by approximately by 0.1 units or so over parts
of continental Europe. The pH increases with diameter by 0.5 units for $\text{PM}_{1-2.5}$, 0.8 units for $\text{PM}_{2.5-5}$
and 1.4 units for PM_{5-10} .

305 The effect of dust on pH and aerosol water is reflected on the predicted aerosol nitrate.
Nitrate in all particle sizes decreases when dust is assumed to be inert (Fig. S8), as the
corresponding pH reduction (for cases when $\text{pH} < 2.5$) does not favor the partitioning of nitrate to
the aerosol phase. The effect of dust on submicrometer nitrate is negligible in most areas, but there
is still an effect in the Netherlands and the surrounding areas (Fig. S8). The dust is predicted to
310 cause average increases of $\text{PM}_{1-2.5}$, $\text{PM}_{2.5-5}$ and PM_{5-10} nitrate up to $0.5 \mu\text{g m}^{-3}$, $1.3 \mu\text{g m}^{-3}$ and $1.2 \mu\text{g m}^{-3}$,
respectively in parts of northern Europe with higher dust levels and also Italy. This nonlinear
impact of relatively minor amounts of NVCs from dust occurs because relatively small changes in
aerosol pH, when occurring in the “pH sensitivity window” of nitrate partitioning can lead to large
responses in nitrate uptake (Vasilakos et al., 2018).

315

4.5.1 The role of calcium

Predicted aerosol water levels decrease in the absence of calcium compared to the base case
simulation (Fig. S9). The increase of aerosol water concentration caused by the calcium ranges
between $0.8\text{-}1 \mu\text{g m}^{-3}$ for PM_1 , $0.8\text{-}1.1 \mu\text{g m}^{-3}$ for $\text{PM}_{1-2.5}$, $0.8\text{-}1.2 \mu\text{g m}^{-3}$ for $\text{PM}_{2.5-5}$ and $0.7\text{-}1.3 \mu\text{g m}^{-3}$
320 PM_{5-10} over continental Europe. The effect is more significant in the coarse particles where
most of the calcium is found. Considering the possible effects calcium can have on soluble sulfate
and water uptake, the simulations suggests that the primary effect of calcium is through its action as
a soluble ion. If calcium is neglected in the simulation, aerosol pH decreases for all particle sizes
compared to the base case simulation (Fig. 8). This decrease varies from 0.2 to 0.3 units for PM_1 ,
325 0.25-0.4 units for $\text{PM}_{1-2.5}$, 0.3-0.5 for $\text{PM}_{2.5-5}$ and 0.6-0.8 for PM_{5-10} over continental Europe. The



highest pH differences are predicted for the coarse particles, consistent with that the coarse particles are richest in calcium.

5. Conclusions

330 The size-dependent aerosol pH was simulated over Europe during an early summer period. We find that fine mode aerosol is persistently more acidic than coarse mode particles. The size-dependence of pH is strongest in northern and southern Europe, where the difference can be as large as 4 units between submicron and 10 μm particles. This difference is reduced over continental regions, but can still be as large as 1 pH unit between PM_1 and $\text{PM}_{1-2.5}$. PM_1 has the most water over continental
335 areas, while $\text{PM}_{2.5-5}$ and PM_{5-10} have the most water in the marine and coastal areas.

Particles of all sizes become increasingly acidic with altitude owing to the reduction of aerosol water levels with height and volatilization of particulate ammonium and nitrate due to dilution. The highest pH decrease between the ground and 2.5 km altitude is 0.5-1 units for PM_1 , 1.5-2 units for $\text{PM}_{1-2.5}$ and $\text{PM}_{2.5-5}$, 1.3 units for PM_{5-10} . The largest drop in pH is observed for the
340 $\text{PM}_{1-2.5}$ fraction because it coincides with where aerosol nitrate resides most – hence its evaporation with altitude tends to have a larger impact on pH than reductions of liquid water from the RH effect alone.

The nitrate concentration tends to peak a few hours later than the pH in all examined sites due to the time required for the production of nitric acid and its partitioning to the aerosol phase. If
345 aerosol pH becomes low enough to impede fine mode nitrate formation, its preferential condensation to larger sizes tends to increase the pH difference across size. The highest average nitrate levels over Europe are predicted for the 2.5-5 μm range for which the average pH is equal to 2.6 during the simulated period.

Dust causes increases of the aerosol water levels in all particle sizes. The increase in water
350 levels ranges from 1 to 6 $\mu\text{g m}^{-3}$ with the highest change for PM_{5-10} in parts of northern Europe with relative high concentrations of dust. Dust also causes an increase in aerosol pH for all particle sizes with higher effects in the coarse particles. This effect can be more than 1 pH unit. This increase in pH is accompanied by increases in aerosol nitrate, which can be as large as 2.5 $\mu\text{g m}^{-3}$. This effect of dust is mainly due to its calcium content, suggesting the importance of simulating accurately not
355 only the dust concentration but also the calcium levels.

This study clearly shows that aerosol acidity and liquid water content changes considerably across size, location, time and height over Europe. These changes will impact aerosol formation and its response to emissions controls, solubility of aerosol trace metals and deposition. With this



realization, aerosol pH and liquid water content emerge as powerful aerosol state variables (Nenes et
360 al., 2019) that could help elucidate the complex impacts of aerosol on public health, ecosystems and
climate.

Acknowledgments. This work was supported by the project PyroTRACH (ERC-2016-COG) funded
from H2020-EU.1.1. - Excellent Science - European Research Council (ERC), project ID 726165.

365

Code and Data availability. Simulation results are available upon request.

Competing interests. The authors declare that they have no conflicts of interest.

370 **Author contributions.** MZ, SN and AN conceived and led the study. MZ developed and
implemented the pH calculation scheme in PMCAMx, carried out the simulations and wrote the first
draft of the paper. SK contributed the dust emissions and NVC scheme. MZ, AN and SP were
involved in the scientific interpretation of the simulations. All authors provided feedback on the
analysis approach and extensively commented on the manuscript.

375

References

- Bougiatioti, A., Nikolaou, P., Stavroulas, I., Kouvarakis, G., Weber, R., Nenes, A., Kanakidou, M.
and Mihalopoulos, N.: Particle water and pH in the eastern Mediterranean: source variability
and implications for nutrient availability, *Atmos. Chem. Phys.*, 16, 4579–4591, 2016.
- 380 Carter, W. P. L.: Documentation of the SAPRC-99 Chemical Mechanism for VOC Reactivity
Assessment. Report to California Air Resources Board. pah.cert.unc.edu/~carter/absts.htm,
2000.
- Ciarelli, G., Aksoyoglu, S., Crippa, M., Jimenez, J., Nemitz, E., Sellegri, K., Äijälä, M., Carbone,
S., Mohr, C., O'Dowd, C., Poulain, L., Baltensperger, U. and Prévôt, A. S. H.: Evaluation of
385 European air quality modelled by CAMx including the volatility basis set scheme, *Atmos.*
Chem. Phys., 16, 10313-10332, 2016.
- Ding, J., Zhao, P., Su, J., Dong, Q., Du, X. and Zhang, Y.: Aerosol pH and its driving factors in
Beijing, *Atmos. Chem. Phys.*, 19, 7939-7954, 2019.
- Environ: User's guide to the comprehensive air quality model with extensions (CAMx), version
390 4.02, report, ENVIRON Int. Corp., Novato, Calif. (available at <http://www.camx.com>), 2003.
- Fang, T., Guo, H., Zeng, L., Verma, V., Nenes, A. and Weber, R. J.: Highly acidic ambient
particles, soluble metals, and oxidative potential: a link between sulfate and aerosol toxicity,
Environ. Sci. Technol., 51, 2611–2620, 2017.
- Fountoukis, C. and Nenes, A.: ISORROPIA II: a computationally efficient thermodynamic



- 395 equilibrium model for K^+ - Ca^{2+} - Mg^{2+} - NH_4^+ - Na^+ - SO_4^{2-} - NO_3^- - Cl^- - H_2O aerosols, *Atmos. Chem. Phys.*, 7, 4639-4659, 2007.
- Fountoukis, C., Racherla, P. N., Denier Van Der Gon, H. A. C., Polymeneas, P., Charalampidis, P. E., Pilinis, C., Wiedensohler, A., Dall'Osto, M., O'Dowd, C. and Pandis, S. N.: Evaluation of a three-dimensional chemical transport model (PMCAMx) in the European domain during the EUCAARI May 2008 campaign, *Atmos. Chem. Phys.*, 11, 10331–10347, 2011.
- 400 Fridlind, A. M. and Jacobson, M. Z.: A study of gas-aerosol equilibrium and aerosol pH in the remote marine boundary layer during the First Aerosol Characterization Experiment (ACE 1), *J. Geophys. Res.*, 105, 17325–17340, 2000.
- Guenther, A., Karl, T., Harley, P., Wiedinmyer, C., Palmer, P. I. and Geron, C.: Estimates of global terrestrial isoprene emissions using MEGAN (Model of Emissions of Gases and Aerosols from Nature), *Atmos. Chem. Phys.*, 6, 3181-3210, 2006.
- 405 Guo, H., Xu, L., Bougiatioti, A., Cerully, K. M., Capps, S. L., Hite, J. R., Carlton, A. G., Lee, S. H., Bergin, M. H., Ng, N. L., Nenes, A. and Weber, R. J.: Fine-particle water and pH in the southeastern United States, *Atmos. Chem. Phys.*, 15, 5211–5228, 2015.
- 410 Guo, H., Sullivan, A. P., Campuzano-Jost, P., Schroder, J. C., Lopez-Hilfiker, F. D., Dibb, J. E., Jimenez, J. L., Thornton, J. A., Brown, S.S., Nenes, A. and Weber, R. J.: Fine particle pH and the partitioning of nitric acid during winter in the northeastern United States, *J. Geophys. Res.*, 121, 10355-10376, 2016.
- Guo, H., Liu, J., Froyd, K. D., Roberts, J. M., Veres, P. R., Hayes, P. L., Jimenez, J. L., Nenes, A. and Weber, R. J.: Fine particle pH and gas-particle phase partitioning of inorganic species in Pasadena, California, during the 2010 CalNex campaign, *Atmos. Chem. Phys.*, 17, 5703–5719, 2017.
- 415 Guo, H., Otjes, R., Schlag, P., Kiendler-scharr, A., Nenes, A. and Weber, R. J.: Effectiveness of ammonia reduction on control of fine particle nitrate, *Atmos. Chem. Phys.*, 18, 12241-12256, 2018.
- 420 Heald, C. L., Collett, J. L., Lee, T., Benedict, K. B., Schwandner, F. M., Li, Y., Clarisse, L., Hurtmans, D. R., Van Damme, M., Clerbaux, C., Coheur, P. F., Philip, S., Martin, R. V. and Pye, H. O. T.: Atmospheric ammonia and particulate inorganic nitrogen over the United States, *Atmos. Chem. Phys.*, 12, 10295–10312, 2012.
- 425 Hu, G., Zhang, Y., Sun, J., Zhang, L., Shen, X., Lin, W. and Yang, Y.: Variability, formation and acidity of water-soluble ions in $PM_{2.5}$ in Beijing based on the semi-continuous observations, *Atmos. Res.*, 145–146, 1–11, 2014.
- Huang, X., Qiu, R., Chan, C. K. and Pathak, R. K: Evidence of high $PM_{2.5}$ strong acidity in ammonia-rich atmosphere of Guangzhou, China: Transition in pathways of ambient ammonia to form aerosol ammonium at $[NH_4^+]/[SO_4^{2-}]=1.5$, *Atmos. Res.*, 99, 488–495, 2011.
- 430 Hsu, Y., Wu, C., Lundgren, D. A. and Birky, B. K.: Size distribution, chemical composition and acidity of mist aerosols in fertilizer manufacturing facilities in Florida, *J. Aerosol Sci.*, 39, 127-140, 2008.
- 435 Im, U., Bianconi, R., Solazzo, E., Kioutsioukis, I., Badia, A., Balzarini, A., Baró, R., Bellasio, R.,



- 440 Brunner, D., Chemel, C., Curci, G., van der Gon, H. D., Flemming, J., Forkel, R., Giordano, L., Jiménez-Guerrero, P., Hirtl, M., Hodzic, A., Honzak, L., Jorba, O., Knote, C., Makar, P. A., Manders-Groot, A., Neal, L., Pérez, J. L., Pirovano, G., Pouliot, G., Jose, R. S., Savage, N., Schroder, W., Sokhi, R. S., Syrakov, D., Torian, A., Tuccella, P., Wang, K., Werhahn, J., Wolke, R., Zabkar, R., Zhang, Y., Zhang, J., Hogrefe, C. and Galmarini, S.: Evaluation of operational online-coupled regional air quality models over Europe and North America in the context of AQMEII phase 2. Part II: Particulate matter, *Atmos. Environ.*, 115, 421-441, 2015.
- 445 Kakavas, S. and Pandis, S. N.: Effects of urban dust emissions on fine and coarse PM nitrate concentrations, *Atmos. Environ.*, submitted for publication, 2020.
- Karydis, V. A., Tsimpidi, A. P., Fountoukis, C., Nenes, A., Zavala, M., Lei, W., Molina, L. T. and Pandis, S. N.: Simulating the fine and coarse inorganic particulate matter concentrations in a polluted megacity, *Atmos. Environ.*, 44, 608–620, 2010.
- 450 Katoshevski, D., Nenes, A. and Seinfeld, J. H.: A study of processes that govern the maintenance of aerosols in the marine boundary layer, *J. Aerosol Sci.*, 30, 503-532, 1999.
- Keene, W. C., Pszenny, A. A. P., Maben, J. R., Stevenson, E. and Wall, A.: Closure evaluation of size-resolved aerosol pH in the New England coastal atmosphere during summer, *J. Geophys. Res.*, 109, 1–16, 2004.
- 455 Kumala, M., Asmi, A., Lappalainen, H. K., Carslaw, K. S., Poschl, U., Baltensperger, U., Hov, Ø., Brenquier, J.-L., Pandis, S. N., Facchini, M. C., Hansson, H.-C., Wiedensohler, A., and O’Dowd, C. D.: Introduction: European Integrated Project on Aerosol Cloud Climate and Air Quality interactions (EUCAARI) – integrating aerosol research from nano to global scales, *Atmos. Chem. Phys.*, 9, 2825–2841, 2009.
- 460 Masiol, M., Squizzato, S., Formenton, G., Khan, Md. B., Hopke, P. K., Nenes, A., Pandis, S. N., Tositti, L., Benetello, F., Visin, F. and Pavoni, B.: Hybrid multiple-site mass closure and source apportionment of PM_{2.5} and aerosol acidity at major cities in the Po Valley, *Sci. Total Environ.*, <https://doi.org/10.1016/j.scitotenv.2019.135287>, 2019.
- Meskhidze, N., Chameides, W. L., Nenes, A. and Chen, G.: Iron mobilization in mineral dust: Can anthropogenic SO₂ emissions affect ocean productivity?, *Geophys. Res. Lett.*, 30, 1–5, 2003.
- 465 Mishra, A. K., Koren, I. and Rudich, Y.: Effect of aerosol vertical distribution on aerosol-radiation interaction: a theoretical prospect, *Heliyon*, doi: 10.1016, 2015.
- Nah, T., Guo, H., Sullivan, A. P., Chen, Y., Tanner, D. J., Nenes, A., Russell, A., Lee Ng, N., Gregory Huey, L. and Weber, R. J.: Characterization of aerosol composition, aerosol acidity, and organic acid partitioning at an agriculturally intensive rural southeastern US site, *Atmos. Chem. Phys.*, 18, 11471–11491, 2018.
- 470 Nenes, A., Krom, M. D., Mihalopoulos, N., Van Cappellen, P., Shi, Z., Bougiatioti, A., Zampas, P. and Herut, B.: Atmospheric acidification of mineral aerosols: a source of bioavailable phosphorus for the oceans, *Atmos. Chem. Phys.*, 11, 6265-6272, 2011.
- 475 Nenes, A., Pandis, S. N., Weber, R. J. and Russell, A.: Aerosol pH and liquid water content determine when particulate matter is sensitive to ammonia and nitrate availability, *Atmos. Chem. Phys. Discuss.*, doi.org/10.5194/acp-2019-840, 2019.



- O'Dowd, C. D., Langmann, B., Varghese, S., Scannell, C., Ceburnis, D. and Facchini, M. C.: A combined organic-inorganic sea-spray source function, *Geophys. Res. Lett.*, 35, L01801, 2008.
- 480 Pathak, R. K., Yao, X., Lau, A. K. H. and Chan, C. K.: Acidity and concentrations of ionic species of PM_{2.5} in Hong Kong, *Atmos. Environ.*, 37, 1113–1124, 2003.
- Pilinis, C., Capaldo, K. P., Nenes, A. and Pandis, S. N.: MADM-A new multicomponent aerosol dynamics model, *Aerosol Sci. Tech.*, 32, 482-502, 2000.
- 485 Pye, H. O. T., Liao, H., Wu, S., Mickley, L. J., Jacob, D. J., Henze, D. K. and Seinfeld J. H.: Effect of changes in climate and emissions on future sulfate-nitrate-ammonium aerosol levels in the United States, *J. Geophys. Res.*, 114, doi:10.1029/2008JD010701, 2009.
- Pye, H. O. T., Nenes, A., Alexander, B., Ault, A. P., Barth, M. C., Clegg, S. L., Collett Jr., J. L., Fahey, K. M., Hennigan, C. J., Herrmann, H., Kanakidou, M., Kelly, J. T., Ku, I.-T., McNeill, V. F., Riemer, N., Schaefer, T., Shi, G., Tilgner, A., Walker, J. T., Wang, T.,
490 Weber, R., Xing, J., Zaveri, R. A., and Zuend, A.: The Acidity of Atmospheric Particles and Clouds, *Atmos. Chem. Phys. Discuss.*, <https://doi.org/10.5194/acp-2019-889>, in review, 2019
- Raizenne, M., Neas, L. M., Damokosh, A. I., Dockery, D. W., Spengler, J. D., Koutrakis, P., Ware, J. H. and Speizer, F. E.: Health effects of acid aerosols on North American children: pulmonary function, *Environ. Health Perspect.*, 104, 506-514, 1996.
- 495 Seinfeld, J. H. and Pandis, S. N.: *Atmospheric Chemistry and Physics. From Air Pollution to Climate Change. Second Edition*, Wiley, New Jersey, 2006.
- Skamarock, W. C., Klemp, J. B., Dudhia, J., Gill, D. O., Barker, D. M., Wang, W. and Powers, J. G.: A description of the advanced research WRF Version 2, NCAR Technical Note (www.mmm.ucar.edu/wrf/users/docs/arw_v2.pdf), 2005.
- 500 Squizzato, S., Masiol, M., Brunelli, A., Pistollato, S., Tarabotti, E., Rampazzo, G. and Pavoni, B.: Factors determining the formation of secondary inorganic aerosol: a case study in the Po Valley (Italy), *Atmos. Chem. Phys.*, 13, 1927-1939, 2013.
- Trump, E. R., Fountoukis, C., Donahue, N. M. and Pandis, S. N.: Improvement of simulation of fine inorganic PM levels through better descriptions of coarse particle chemistry, *Atmos. Environ.*, 102, 274–281, 2015.
- 505 Tsimpidi, A. P., Karydis, V. A., Zavala, M., Lei, W., Molina, L., Ulbrich, I. M., Jimenez, J. L. and Pandis, S. N.: Evaluation of the volatility basis-set approach for the simulation of organic aerosol formation in the Mexico City metropolitan area, *Atmos. Chem. Phys.*, 10, 525–546, 2010.
- 510 Tuccella, P., Curci, G., Visconti, G., Bessagnet, B., Menut, L. and Park, R. J.: Modeling of gas and aerosol with WRF/Chem over Europe: evaluation and sensitivity study, *J. Geophys. Res.*, 117, doi:10.1029/2011JD016302, 2012.
- Vasilakos, P., Russell, A., Weber, R. and Nenes, A.: Understanding nitrate formation in a world with less sulfate, *Atmos. Chem. Phys.*, 18, 12765-12775, 2018.
- 515 Visschedijk, A. J. H., Zandveld, P. and Denier van der Gon, H. A. C.: TNO Report 2007 A-R0233/B: A high resolution gridded European emission database for the EU integrated



- project GEMS, Netherlands, Organization for Applied Scientific Research, 2007.
- Walker, J. M., Philip, S., Martin, R. V. and Seinfeld, J. H.: Simulation of nitrate, sulfate and ammonium aerosols over the United States, *Atmos. Chem. Phys.*, 12, 11213-11227, 2012.
- 520 Wang, H., Sun, Z., Li, H., Gao, Y., Wu, J. and Cheng, T.: Vertical distribution characteristics of atmospheric aerosols under different thermodynamic conditions in Beijing, *Aerosol and Air Quality Res.*, 18, 2775-2787, 2018.
- Weber, R. J., Guo, H., Russell, A. G. and Nenes, A.: High aerosol acidity despite declining atmospheric sulfate concentrations over the past 15 years, *Nat. Geosci.*, 9, 1–5, 2016.
- 525 Xue, J., Lau, A. K. H. and Yu, J. Z.: A study of acidity on $PM_{2.5}$ in Hong Kong using online ionic chemical composition measurements, *Atmos. Environ.*, 45, 7081–7088, 2011.
- Yu, S., Dennis, R., Roselle, S., Nenes, A., Walker, J., Eder, B., Schere, K., Swall, J. and Robarge, W.: An assessment of the ability of three-dimensional air quality models with current thermodynamic equilibrium models to predict aerosol NO_3^- , *J. Geophys. Res.*, 110, <https://doi.org/10.1029/2004JD004718>, 2005.
- 530 Zakoura, M. and Pandis, S. N.: Overprediction of aerosol nitrate by chemical transport models: The role of grid resolution, *Atmos. Environ.*, 187, 390-400, 2018.
- Zakoura M. and Pandis, S. N.: Improving fine aerosol nitrate predictions using a Plume-in-Grid modeling approach, *Atmos. Environ.*, 215, 116887, 2019.
- 535



540

545

550

555

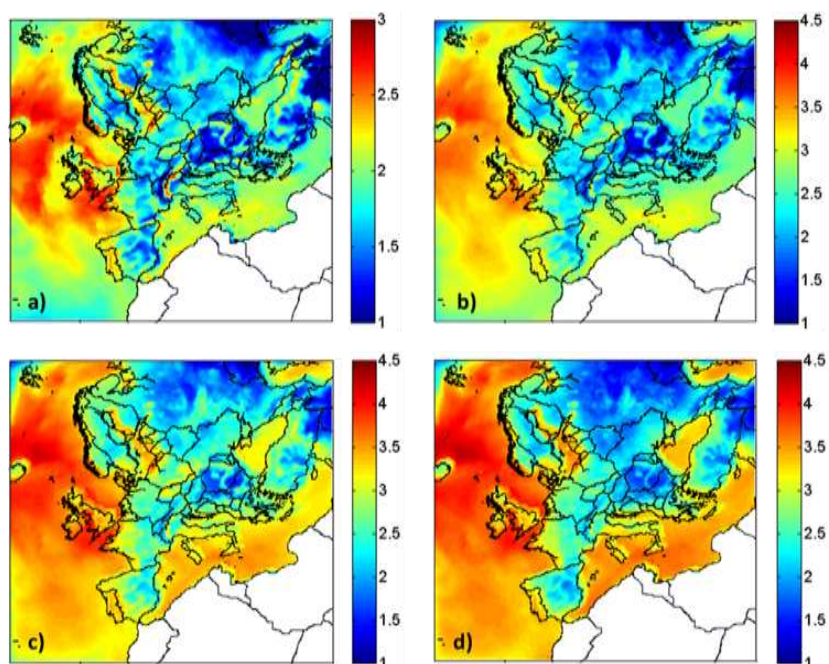


Figure 1. Average ground level aerosol pH predictions for **a)** PM_{1} , **b)** $PM_{1-2.5}$, **c)** $PM_{2.5-5}$ and **d)** PM_{5-10} for the base case simulation over Europe during May 2008.

560

565

570



575

580

585

590

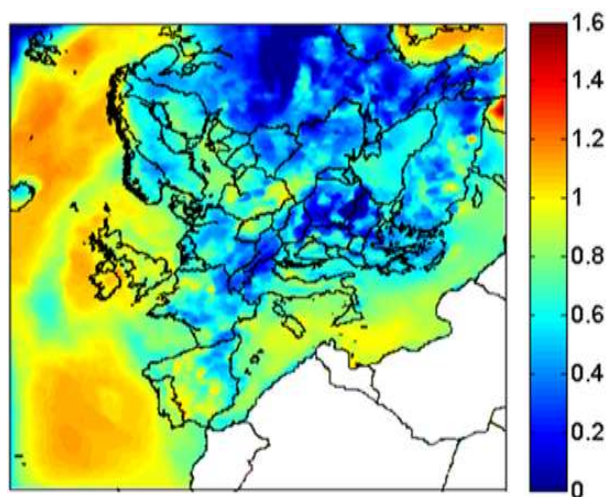


Figure 2. Absolute difference of average ground level pH between PM_{1-2.5} and PM₁ for the base case simulation during May 2008.

595

600

605

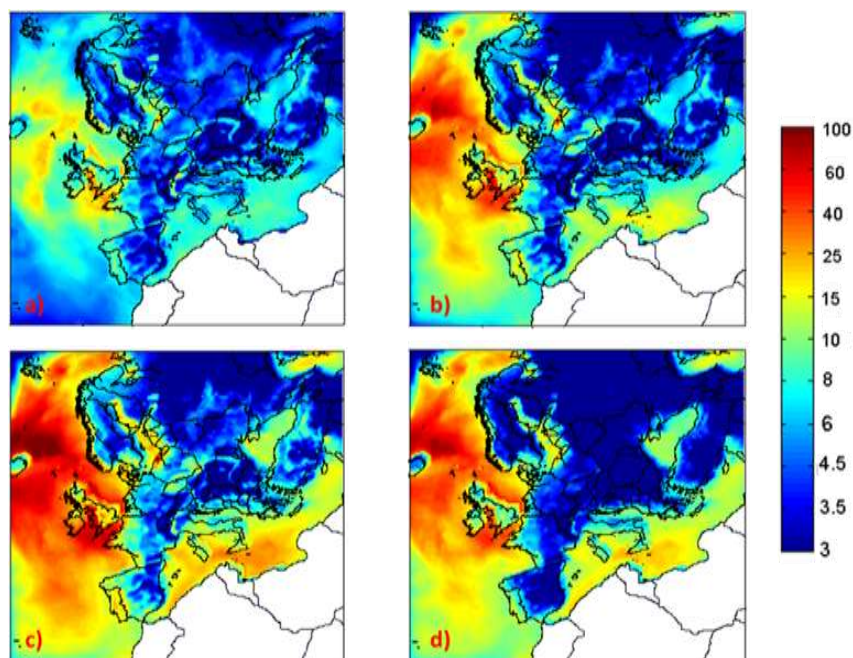


610

615

620

625



630

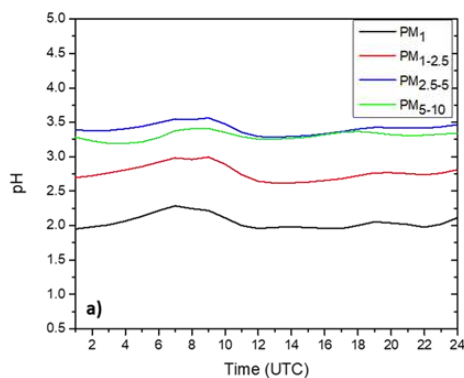
Figure 3. Average ground level aerosol water predictions (in $\mu\text{g m}^{-3}$) for **a)** PM_{1} , **b)** $\text{PM}_{1-2.5}$, **c)** $\text{PM}_{2.5-5}$ and **d)** PM_{5-10} for the base case simulation over Europe during May 2008.

635

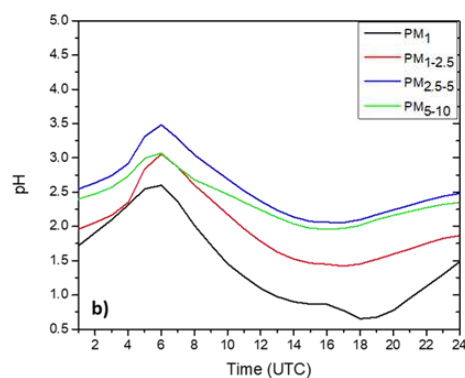
640



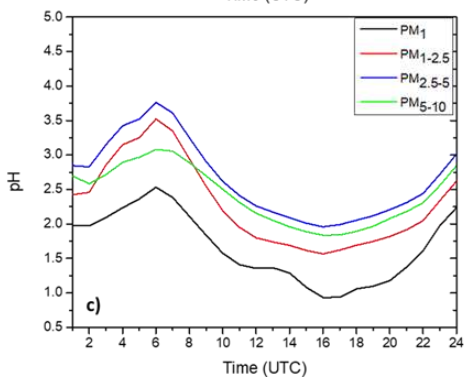
645



650



655



660

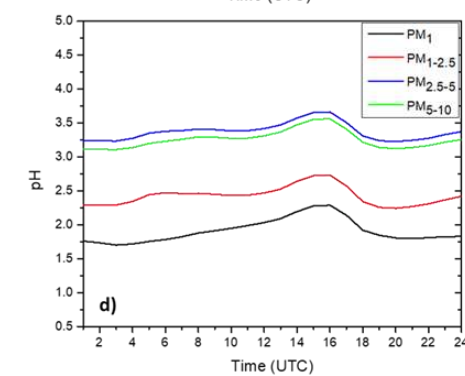


Figure 4. Average pH diurnal profiles for **a)** Cabauw, Netherlands, **b)** Melpitz, Germany, **c)** Paris, France and **d)** Finokalia, Greece for the four particle size ranges for the base case simulation during May 2008.

670



675

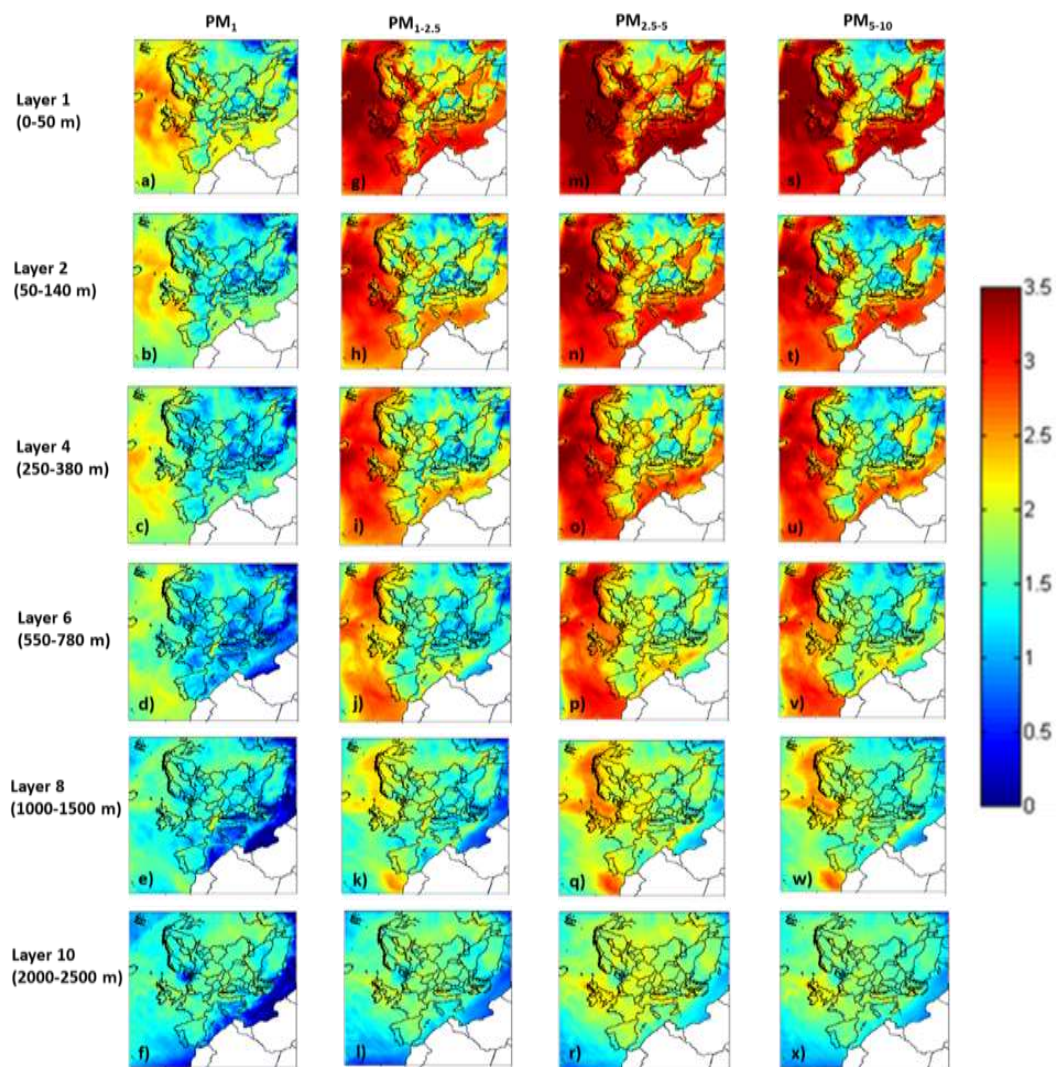
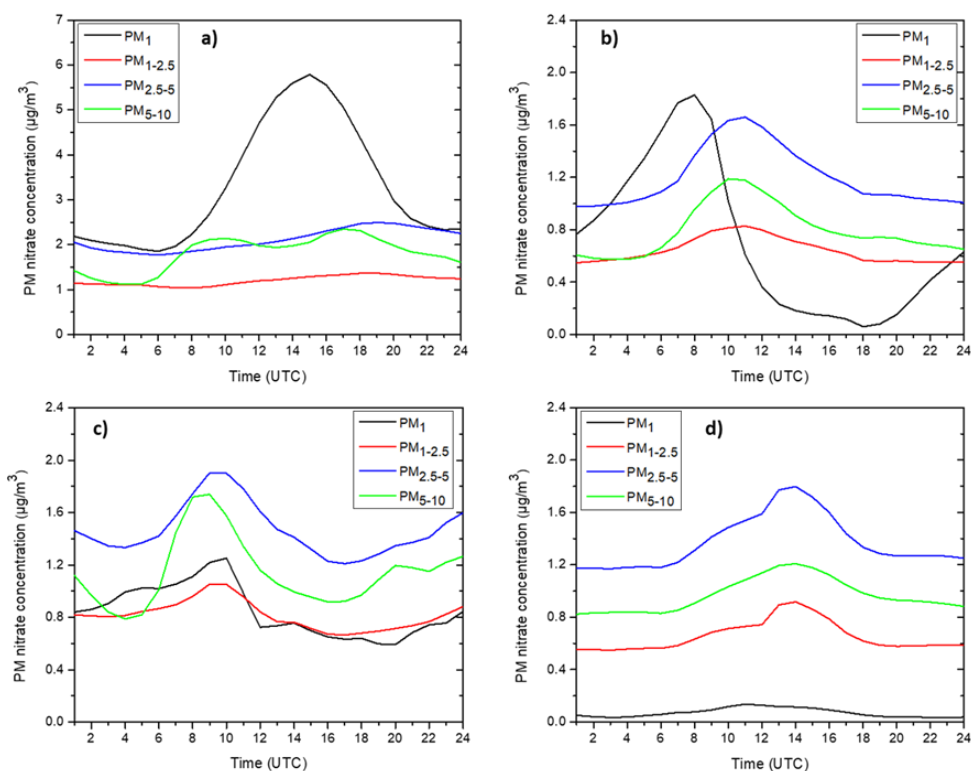


Figure 5. Average predicted aerosol pH as a function of size and altitude: **a), b), c), d), e), f)** for PM_{1} , **g), h), i), j), k), l)** for $PM_{1-2.5}$, **m), n), o), p), q), r)** for $PM_{2.5-5}$, **s), t), u), v), w), x)** for PM_{5-10} at 0-50 m, 50-140 m, 250-380 m, 550-780 m, 1000-1500 m, and 2000-2500 m for the base case simulation during May 2008.

685

21



690

Figure 6. PM_1 , $\text{PM}_{1-2.5}$, $\text{PM}_{2.5-5}$ and PM_{5-10} nitrate diurnal profiles for **a)** Cabauw, Netherlands, **b)** Melpitz, Germany, **c)** Paris, France and **d)** Finokalia, Greece for the base case simulation during May 2008.

695

700



705

710

715

720

725

730

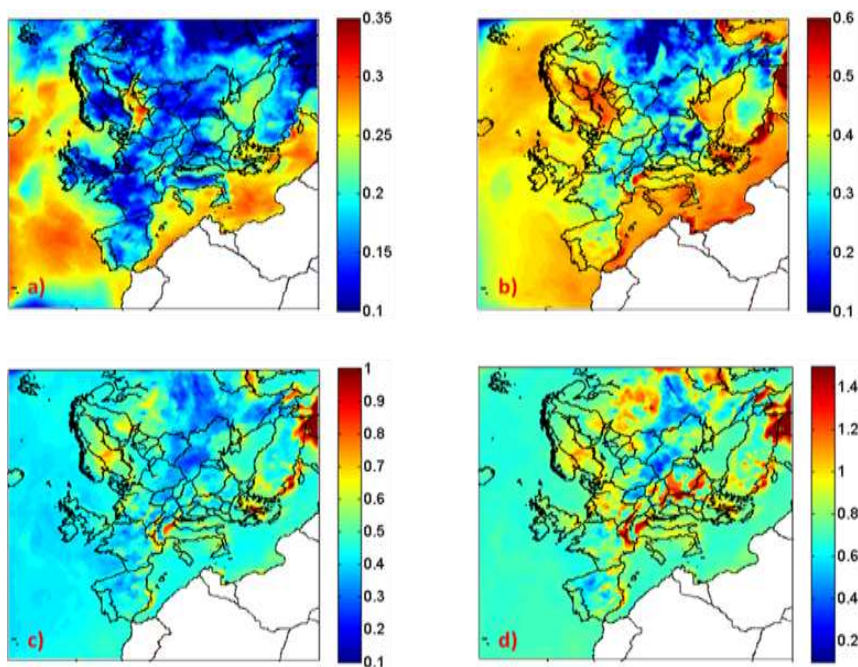
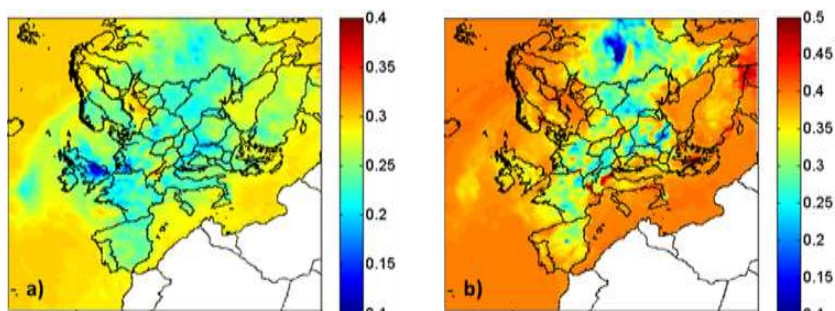


Figure 7. Increase of average ground level aerosol pH for **a)** PM₁, **b)** PM_{1-2.5}, **c)** PM_{2.5-5} and **d)** PM₅₋₁₀ for the base case simulation compared to the inert dust case during May 2008.

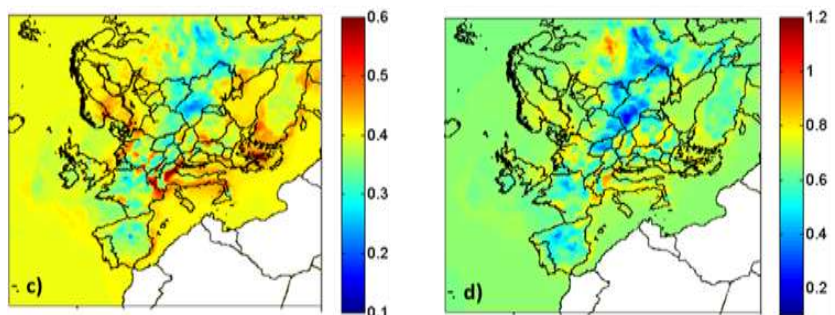


735

740



745



750

755

Figure 8. Increase of average ground level aerosol pH for a) PM_{1} , b) $PM_{1-2.5}$, c) $PM_{2.5-5}$ and d) PM_{5} for the base case simulation compared to the case when calcium is neglected during May 2008.